

Microglia secrete miR-146a-5p-containing exosomes to regulate neurogenesis in depression

Cuiqin Fan,¹ Ye Li,¹ Tian Lan,¹ Wenjing Wang,¹ Yifei Long,¹ and Shu Yan Yu^{1,2}

¹Department of Physiology, School of Basic Medical Sciences, Cheeloo College of Medicine, Shandong University, Jinan, Shandong 250012, China; ²Shandong Provincial Key Laboratory of Mental Disorders, School of Basic Medical Sciences, Cheeloo College of Medicine, Shandong University, Jinan, Shandong 250012, China

Enhancing neurogenesis within the hippocampal dentate gyrus (DG) is critical for maintaining brain development and function in many neurological diseases. However, the neural mechanisms underlying neurogenesis in depression remain unclear. Here, we show that microglia transfer a microglia-enriched microRNA, miR-146a-5p, via secreting exosomes to inhibit neurogenesis in depression. Overexpression of miR-146a-5p in hippocampal DG suppresses neurogenesis and spontaneous discharge of excitatory neurons by directly targeting Krüppel-like factor 4 (KLF4). Downregulation of miR-146a-5p expression ameliorates adult neurogenesis deficits in DG regions and depression-like behaviors in rats. Intriguingly, circular RNA ANKS1B acts as a miRNA sequester for miR-146a-5p to mediate post-transcriptional regulation of KLF4 expression. Collectively, these results indicate that miR-146a-5p can function as a critical factor regulating neurogenesis under conditions of pathological processes resulting from depression and suggest that microglial exosomes generate new crosstalk channels between glial cells and neurons.

INTRODUCTION

Depression, one of the most common psychiatric disorders, typically consists of symptoms involving anhedonia, pessimism, loss of appetite, and insomnia.¹ Understandably, these symptoms seriously affect and reduce the quality of life in these individuals. Depression is a recurrent lifelong condition with a complicated pathogenesis.² Current clinical antidepressant treatments have a poor prognosis, and newly developed drugs show a high failure rate in clinical trials.³ Therefore, the identification of new targets for the treatment of depression represents an essential area of investigation.

Results from previous studies have indicated that the pathophysiological processes of depression are closely related to neurotransmitter changes, an abnormal hypothalamic-pituitary-adrenal (HPA) axis and/or inflammation.⁴ In patients with depression, the volume of the hippocampus was found to be significantly decreased,⁵ an effect often positively correlated with the duration of depression.^{6–9} In addition, the size and density of neurons and glial cells in the dorsolateral prefrontal cortex were also decreased in depression.¹⁰ As most antidepressants work by increasing neurogenesis in the adult brain,¹¹ the identification of novel targets for the induction of neurogenesis suggests a new direction for research into therapeutic strategies for use in the treatment of depression.

Exosomes, which are a type of vesicle with a double membrane structure, can carry a variety of molecules, such as specific microRNAs, DNA, mRNA, and proteins, to recipient cells.¹² The capacity for transport of exosomes across the blood-brain barrier enables them to play a key role in cellular communication, neurogenesis, and synaptic plasticity in the central nervous system.^{13,14} A diverse array of cells, including microglia, can secrete exosomes.¹⁵ A previous study has reported that microglia participate in stem cell proliferation and survival through their release of important trophic factors and anti-inflammatory cytokines.¹⁶ In addition, it has been reported that microglia can secrete exosomes carrying miRNA that are capable of exerting an acute impact upon adult neuroplasticity.^{17,18} In this way, microglia are considered as active regulators of adult neurogenesis,¹⁹ and these microglia appear to perform this function at least by secreting exosomes to promote inter-neuronal communication.²⁰ However, to the best of our knowledge there are no reports on the impact of exosomes and their cargo as related to the development of depression.

MicroRNAs (miRNAs) are non-coding RNAs comprised of 18–24 nucleotides that regulate gene expression by directly modifying messenger RNA (mRNA) after transcription.²¹ miRNAs have been shown to be abundantly expressed in the brain, and miRNA dysfunction contributes to neurological diseases.^{22,23} For example, levels of miR-133b are decreased in the midbrain of Parkinson's disease patients.²⁴ Furthermore, of particular relevance to the present investigation, recent evidence has emerged indicating that miRNAs are important participants in the pathogenesis of depression.²⁵ Results from clinical studies have revealed that various miRNA alterations are present in cerebrospinal fluid, serum, and the ventral prefrontal cortex in patients with major depression disorder (MDD).²⁶ Thus, clarifying the mechanisms of miRNA regulation in the neurogenesis of depression, may provide new therapeutic strategies for patients with depression.

In this study, we investigated the capacity for microglial transfer of miRNA to neurons through secretion of exosomes as a possible contributing factor impacting neurogenesis in the pathology of depression.

Received 25 July 2021; accepted 3 November 2021;
<https://doi.org/10.1016/j.jmthe.2021.11.006>.

Correspondence: Shu Yan Yu, Department of Physiology, School of Basic Medical Sciences, Cheeloo College of Medicine, Shandong University, Jinan, Shandong 250012, China.

E-mail: shuyanyu@sdu.edu.cn

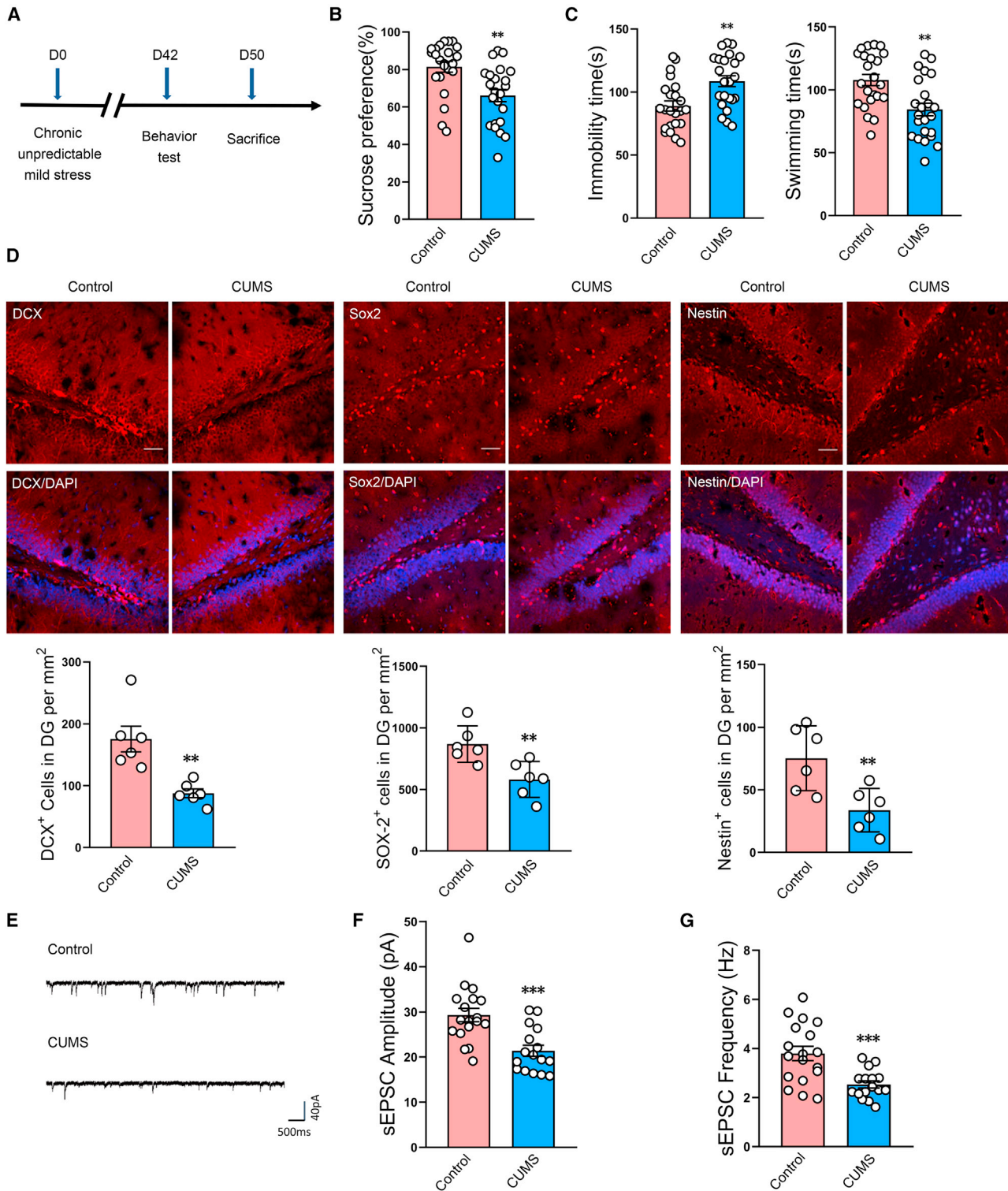


Figure 1. Neurogenesis is reduced in DG regions of CUMS rats

(A) Schematic diagram of experimental design. (B and C) Rats were assessed for depression-like behaviors in the sucrose preference test (SPT) (B) and forced swim test (FST) (C) after 5 weeks of CUMS exposure. n = 23 per group. **p < 0.01 CUMS versus control. (D) Representative confocal microscopic images of immunostainings for Sox2⁺, DCX⁺, and Nestin⁺ cells in DG regions of the hippocampus. Scale bars, 50 μ m. n = 6 per group. **p < 0.01 CUMS versus control. (E) Representative post-synaptic current

(legend continued on next page)

With use of the chronic unpredictable mild stress (CUMS)-induced rat model of depression, we found that levels of miR-146a-5p in microglia-derived exosomes were markedly increased in these rats. miR-146a-5p-enriched exosomes transferred their miR-146a-5p cargo to dentate gyrus (DG)²⁷ neurons of the hippocampus, resulting in an upregulation of miR-146a-5p in DG regions and subsequent downregulation of the miR-146a-5p neurogenesis target, Krüppel-like factor 4 (KLF4). Such effects can exert a substantial impact on neurogenesis. In addition, we found that circular RNA ANKS1B could function as a sequester for miR-146a-5p to affect neurogenesis in depression.

RESULTS

Neurogenesis is reduced in the hippocampal DG of CUMS rats

We first evaluated the behavior of rats subjected to CUMS as assessed in the sucrose preference and forced swim tests (Figure 1A). After 5 weeks of CUMS exposure, the percent of sucrose consumption in the sucrose preference test was significantly reduced, and immobility times in the forced swim test were significantly increased, in these CUMS-exposed rats compared with that of the control group (Figures 1B and 1C). These results verify that this CUMS protocol effectively induced depression-like behavior in these rats. In these CUMS rats, we found a significant reduction of newly developed cells in the DG region (Figure 1D). Moreover, the amplitude and frequency of spontaneous excitatory post-synaptic current (sEPSC) were markedly decreased in DG neurons of hippocampal slices in depressed versus control rats (Figures 1E–1G). These findings suggest that neurogenesis contributes to the pathological processes of depression.

MiR-146a-5p is upregulated in serum-derived exosomes of CUMS rats

Exosomes were isolated from rat serum by ultracentrifugation and precipitation separation to determine whether they may be associated with neurogenesis in this CUMS model of depression. These vesicles possessed a double membrane structure (Figure 2A) and a median diameter of 91.28 nm (Figure 2B), characteristics which were suggestive of exosomes. In further support of this conclusion were the findings that high expressions of the exosomal marker proteins, CD63, CD81, and Alix, were present in these vesicles. Meanwhile, poor levels of GM130 and albumin, markers of Golgi apparatus and lipoproteins, respectively, were detected by western blots (Figures 2C, S1, and S2).

It had been reported that miRNAs were enriched in exosomes. As a means to identify critical miRNAs in exosomes that may be involved with the neurogenesis related to the pathology of depression, exosomes were isolated from the serum of CUMS rats and subjected to miRNA high-throughput sequencing. A heatmap showed that various miRNAs were significantly dysregulated in samples from CUMS versus control rats (Figures 2D and S3; and Table S1). We then selected miRNAs with significant changes, such as miR-146a-

5p, miR-122-5p, miR-133a-3p, miR-206-3p, miR-187-3p, and miR-1b for further analysis by quantitative polymerase chain reaction (qPCR) analysis. Levels of these miRNAs matched well with that of the high-throughput sequencing data (Figure 2E). Notably, miR-146a-5p was identified as being most closely related to signaling pathways regulating pluripotency of stem cells (Figure 2F). Therefore, miR-146a-5p was selected as the focus of our current research.

In addition to serum-derived exosomes, we verified the expression of miRNA in DG regions of the hippocampus, a key brain region for adult neurogenesis, with use of high-throughput sequencing and qPCR (Figure S4A). Interestingly, levels of miR-146a-5p were consistent with miRNA sequencing among upregulated miRNAs (Figure S4B). In addition, the presence of miR-146a-5p in CSF showed increased levels of expression in CUMS rats as compared with that in the control group (Figure S4C).

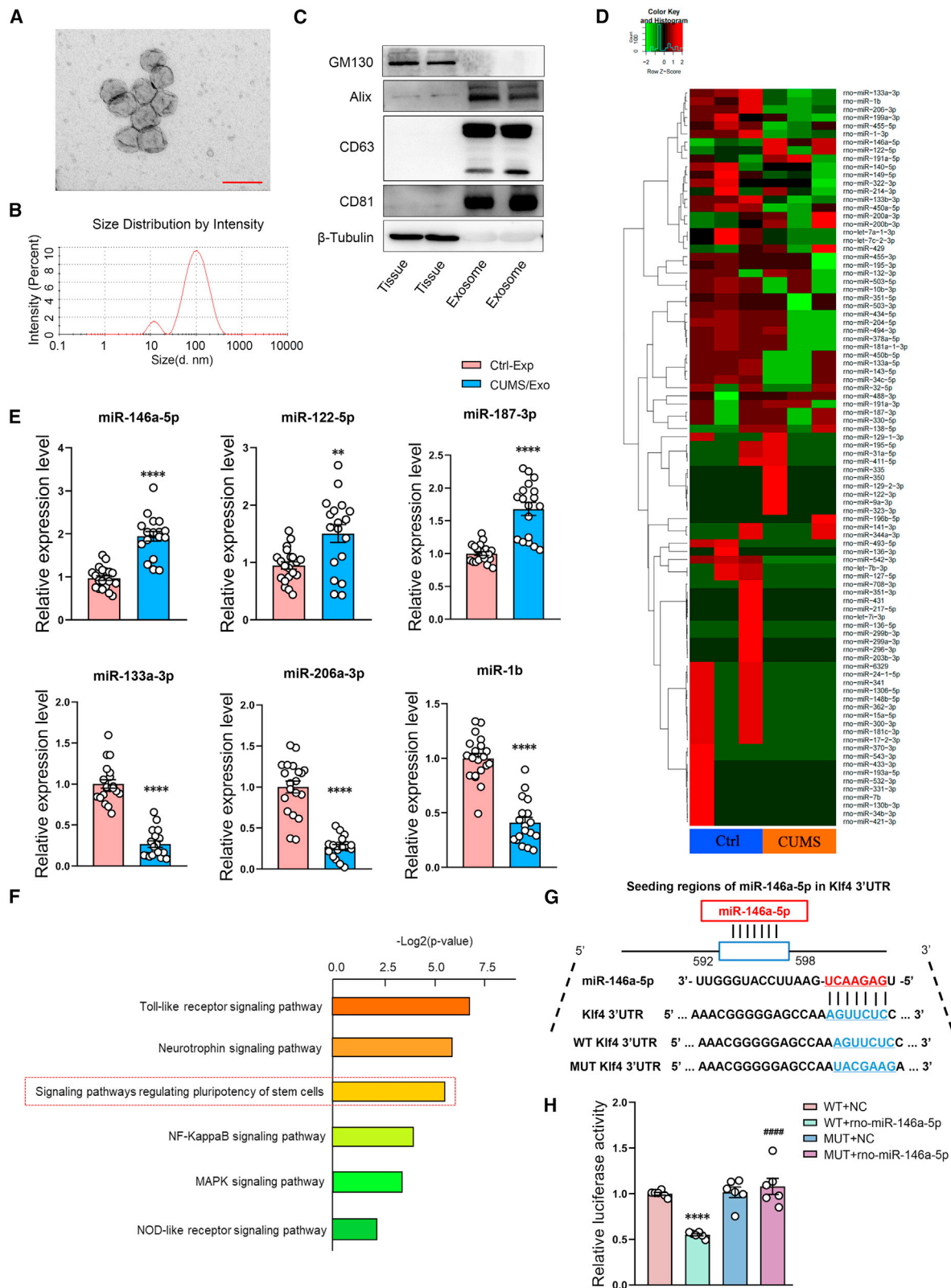
After establishing that CUMS exposure altered levels of miR-146a-5p and that miR-146a-5p was closely related with nervous system development, we next directed our efforts to the identification of potential targets for miR-146a-5p. A total of 27 miR-146a-5p regulated genes were found to be significantly correlated with nervous system development (Figure S5). One eukaryotic transcription factor, which is expressed in neuronal stem cells (NSCs) and regulates neuronal differentiation and migration in the brain, is that of KLF4.²⁸ Results from the luciferase reporter assay demonstrated that miR-146a-5p repressed reporter activity of the transcript containing the wild-type 3' UTR of KLF4, providing further evidence that miR-146a-5p can directly regulate the expression of KLF4 mRNA (Figures 2G and 2H).

Exosomes transfer microglia-derived miR-146a-5p to DG neurons and inhibit the proliferation and differentiation of NSCs

A previous study reported that miR-146a-5p is a microglia-enriched miRNA, not present in hippocampal neurons, and expressed at much lower extent in astrocytes.²⁹ Thus, miR-146a-5p appeared to be shuttling from glia-to-neuron through exosomes. PCR results confirmed that miR-146a-5p is present in cultured microglia and exosomes thereof, more abundantly under stimulation of LPS. Conversely, miR-146a-5p was undetectable in cultured hippocampal neurons, as well as expressed much lower in astrocytes than that in microglia (Figure S6). More important, there was a dramatic increase of miR-146a-5p in exosomes secreted by BV2 cells that were treated with LPS (Figure 3A). Furthermore, we have sorted and collected microglial, neuronal, and astroglial cells individually from dissociated brain tissue by flow cytometry and verified that miR-146a-5p is highly enriched in the microglia (Figure S7).

Considering that CD13 expression is an important feature of microglial exosomes, we wanted to determine whether CD13 levels are

(sEPSC) from whole-cell recordings of spontaneous excitatory activity of DG neurons in control and CUMS rats. (F–G) Cumulative fraction plots of sEPSC amplitudes (F) and frequencies (G) of DG neurons in control and CUMS rats. $n = 18$ neurons from 7 control rats and $n = 16$ neurons from 6 CUMS rats. *** $p < 0.001$ CUMS versus control. Data represent means \pm SEM. Student's t tests for comparisons between the two groups (B–D, F, and G).



(legend on next page)

changed on the surface of these exosomes in response to depression. We found that substantial increases in CD13 levels were present on the surface of serum-derived exosomes in the CUMS versus control groups of rats. In addition, increased expression levels of other microglial-exosome markers, such as MCT-1, CD14, IL-1 β , TMEM119, and CD11b, indicates that the exosomes we collected from serum are mainly of microglial origin (Figure 3B). Next, we further used CSF1R inhibitor (PLX3397) to eliminate microglial cells of rats. As expected, treatment with PLX3397 caused a significant decrease in expression of miR-146a-5p in serum-derived exosomes and DG tissues, confirming that exosomes in serum of CUMS rats were mainly derived from microglia, which may enrich miR-146a-5p (Figure S8). As microglia can transfer functional molecules to neurons via secreted exosomes,²⁰ we next labeled serum-derived exosomes with KH67 (Figure S9A). The presence of green fluorescence-positive labels observed in these DG neurons (Figures 3C and S9B) suggested that the vesicles can be taken up by cells. These results suggested that it is possible that miR-146a-5p may be delivered to neurons to affect the proliferation and differentiation of NSCs.

To investigate whether exosomes transfer miR-146a-5p to neurons to affect neurogenesis, the effect of microglia-derived exosomes containing miR-146a on neuronal proliferation and migration were then investigated *in vitro* in cultured NSCs (Figure S10A). As shown in Figures 3D–3F, the exosomes derived from BV-2 cells which were treated with LPS significantly reduced neuronal proliferation and migration of NSCs when co-culture with these NSCs. Conversely, when BV-2 cells were pretreated with GW4869, an inhibitor of vesicle formation, the decreases in neuronal proliferation (Figure S10B) and migration (Figures S10C and S10D) in NSCs were prevented, indicating an inhibition in the secretion of exosomes containing miR-146a-5p significantly increased neuronal proliferation and migration of NSCs. Moreover, we performed the lentiviral transfection experiments to knock out miR-146a-5p in BV2 cells before LPS treatment, and found that the exosomes derived from these BV2 cells have no inhibitory effect on neurogenesis (Figure S11). Taken together, these data indicate that exosomes derived from microglia can deliver miR-146a-5p to neurons to regulate neurogenesis.

MIR-146a-5p suppresses neurogenesis via the KLF4/CDKL5 pathway

An AAV-miR-146a-5p virus was constructed to overexpress miR-146a-5p within the DG of normal rats or block miR-146a-5p in

CUMS rats (Figures 4A and 4B). Two weeks after virus injection, significant amounts of green fluorescence were present in the DG region (Figure 4C) and miR-146a-5p expression at this site was significantly upregulated in normal rats or downregulated in CUMS rats (Figures S12A and S12B). While CUMS treatment decreased sucrose preferences (Figure 4D) and increased the immobility times (Figure 4E), these effects were essentially reversed following the downregulation of miR-146a-5p in these CUMS rats. In contrast, the overexpression of miR-146a-5p in normal rats resulted in the display of behavioral responses indicative of a depression-like phenotype.

The effects of these AAV-miR-146a-5p virus treatments on neurogenesis in DG neurons were also assessed. In normal rats treated with AAV-miR-146a-5p to overexpress miR-146a-5p, the number of newly developed cells were all significantly reduced (Figures 4F and S12C) as were sEPSC frequencies and amplitudes (Figures 4G–4I). Conversely, the number of new neurons and sEPSC amplitudes and frequencies were significantly increased in CUMS rats receiving AAV-miR-146a-5p-shRNA to downregulate miR-146a-5p.

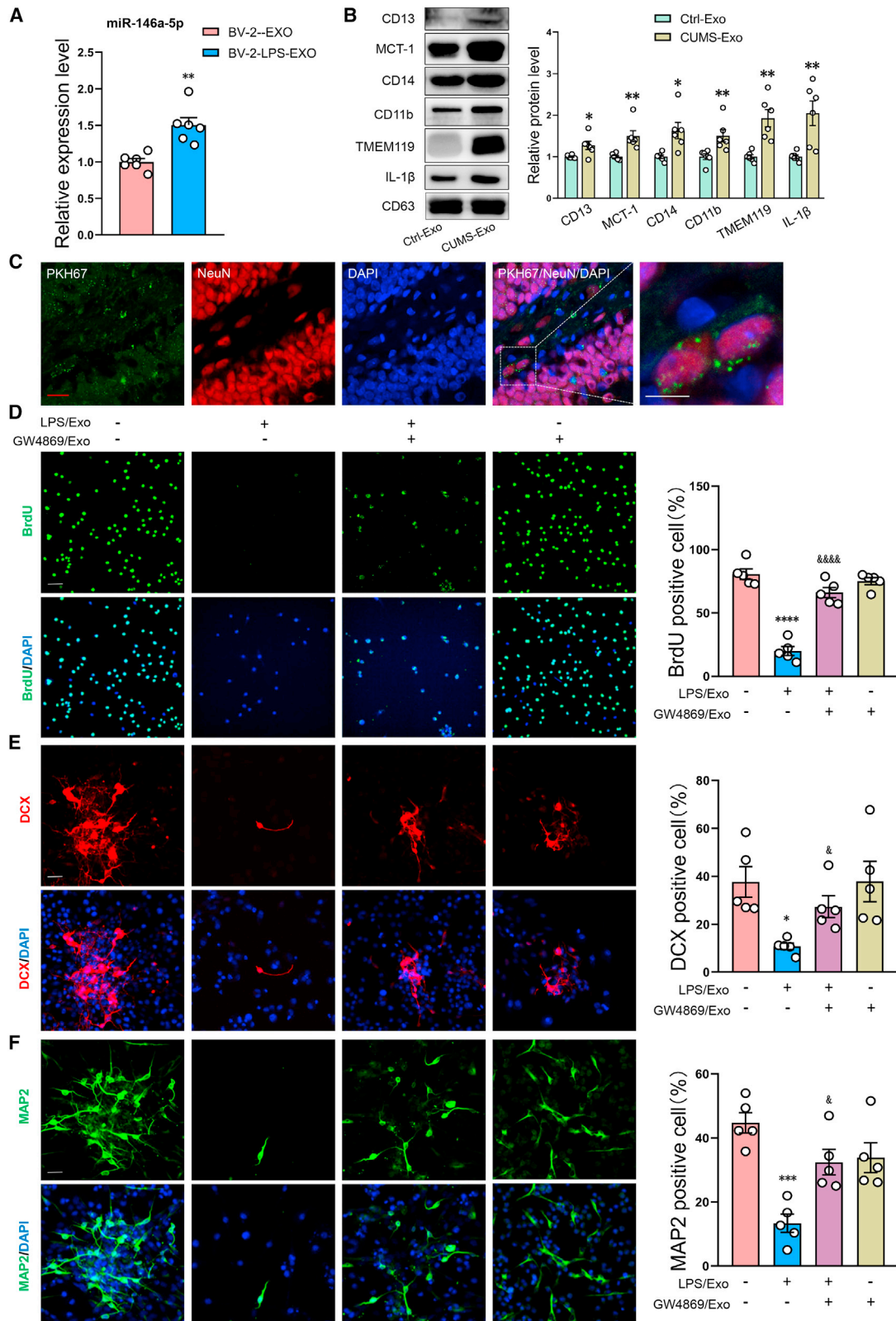
We next sought to investigate some of the downstream molecular mechanisms through which miR-146a-5p may regulate DG neurogenesis. Given that miR-146a-5p directly regulates KLF4 expression, we determined the protein levels of KLF4 in the DG region of these AAV-miR-146a-5p virus-treated rats. The microinjection of miR-146a-5p in normal rats significantly decreased KLF4 and Cdk5 protein expression, while phosphorylation levels of STAT3 were notably increased (Figure 4J). This KLF4 can directly target the phosphorylated form of STAT3 (p-STAT3) and inhibit its expression,³⁰ while Cdk5 contributes to the formation of new granular neurons.³¹ Within the CUMS group, expressions of Klf4 and Cdk5 were all significantly increased, but levels of phosphorylated Stat3 were significantly decreased within DG areas following AAV-miR-146a-5p-shRNA (Figure 4K). These results demonstrate that miR-146a-5p affected neurogenesis in DG neurons via the KLF4/CDKL5 pathway.

KLF4 is necessary for neurogenesis and alleviates depression-like phenotypes in rats

To assess whether a downregulation of KLF4 contributes to the inhibition of neurogenesis as associated with the development of depression, AAV-KLF4-shRNA was injected bilaterally into the DG of normal rats (Figures 5A and 5B). A marked decrease in the protein expression of KLF4 was observed at 2 weeks after AAV-KLF4-shRNA

Figure 2. miR-146a-5p is upregulated in serum-derived exosomes of CUMS rats

(A) Representative transmission electron microscopy images of rat serum-derived exosomes. Scale bar, 200 nm. n = 6 per group. (B) Representative nanoparticle tracking analysis of exosomes derived from rat serum. n = 6 per group. (C) Representative western blot images of relative protein levels for CD63, CD81, Alix, GM130, and β -tubulin in rat serum-derived exosomes. n = 5 per group. (D) Heatmap of miRNAs expressed in exosomes derived from control and CUMS rat serum. n = 3 per group. (E) Relative expression levels of miR-146a-5p, miR-122-5p, miR-187-3p, miR-133a-3p, miR-206-3p, and miR-1b in exosomes obtained from control and CUMS rat serum. SnRNAU6 as the internal controls. Control, n = 20; CUMS, n = 18. **p < 0.01, ****p < 0.0001 CUMS-Exo versus Ctrl-Exo. (F) Bar graphs represent magnitudes of significant correlations for miR-146a-5p-mediated signaling pathways as indicated by respective p values (–log₂ scaled). (G and H) Predicted putative seed-matching sites between miR-146a-5p and KLF4 (G) and Luciferase reporter assay results as performed on 293T cells to detect relative luciferase activities of WT and MUT KLF4 reporters (H). n = 6 per group. #####p < 0.0001 WJUT + rno-miR-146a-5p versus WT + rno-miR-146a-5p, ****p < 0.0001 WT + rno-miR-146a-5p versus WT + NC. Data represent means \pm SEM. Student's t tests for comparisons between the two groups (E). One-way ANOVA with Tukey's post hoc test for multiple comparisons involving >2 groups (F). WT, wild type; MUT, mutation; NC, normal control; Ctrl, control.



(legend on next page)

injection (Figure 5C). These AAV-KLF4-shRNA injected rats displayed behavioral responses characteristic of depression as indicated by decreases in their sucrose preference and significant increases in immobility times (Figures 5D and 5E). As shown in Figure 5F, knockdown of KLF4 expression resulted in significant anti-neurogenesis effects as the number of newly developed cells within the hippocampal DG region were reduced. In addition, protein levels of Cdkl5 were significantly decreased, while phosphorylation levels of STAT3 greatly increased (Figure 5G).

CircANKS1B is decreased in the DG region of CUMS rats and regulates neurogenesis via the miR-146a-5p/KLF4 pathway

As circRNAs mainly function as miRNA “sequesters” to inhibit miRNA activity,³² we were interested in determining the key circRNAs that might be involved with regulating miR-146a-5p expression. Results obtained from the transcriptome sequencing of circRNA expression within DG regions of CUMS rat revealed that statistically significant differences in circRNA expression were present as compared with that in control rats (Figures S13A–S13C). A substantial downregulation in circANKS1B was observed in these rats (Figures S13D and S13E) and, as expected, circANKS1B bound miR-146a-5p through miRNA seed sequence matching (Figure S13F).

To follow up on these findings, we next used AAV2/5 viral vectors to knock down or overexpress circANKS1B levels within the DG region as a means to assess the role of circANKS1B in the depression (Figures S14A–S14C). The markedly increased levels of circANKS1B in rats receiving AAV-circANKS1B and decreased levels in those receiving AAV-circANKS1B-shRNA verified that a high transfection efficiency was present in the DG (Figures S14D and S14E). Within normal rats, AAV-circANKS1B-shRNA treatment increased the levels of miR-146a-5p (Figure 6A). Following knockdown of circANKS1B in the DG, protein levels of KLF4 and CDKL5 were significantly reduced, phosphorylation levels of STAT3 were notably increased (Figures 6B and S15A), while AAV-circANKS1B treatment significantly increased KLF4 and CDKL5 expression, and induced phosphorylation levels of STAT3 (Figures 6C and S15B). Accordingly, it appears that circANKS1B regulates neurogenesis within the DG by affecting the expression of miR-146a-5p. This conclusion follows from the findings that neurogenesis in the circANKS1B-shRNA-infected DG area was reduced, while the overexpression of circANKS1B in the DG of CUMS rats increased the number of newly developed cells (Figure 6D). Furthermore, as shown in Figures 6E and 6F, cir-

cANKS1B can exert corresponding effects upon regulating depression-like behaviors in rats. These results suggest that circANKS1B can function as a sequester for miR-146a-5p to regulate the translational expression of KLF4, thus participating in the neurogenesis associated with depression.

DISCUSSION

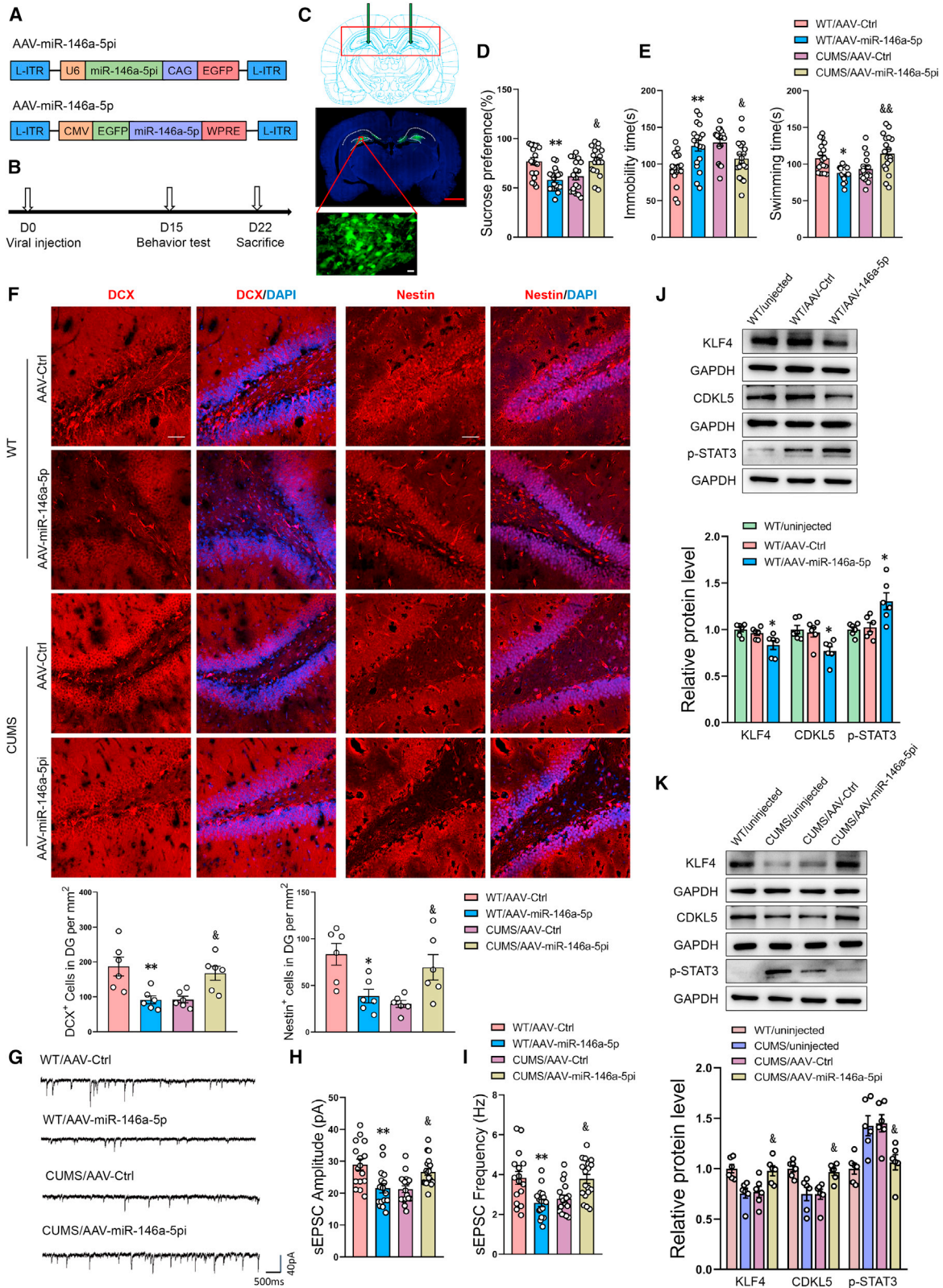
In this study, we provide the first evidence indicating that microglia-specific miR-146a-5p may be a key factor involved in depression and unravel a previously unrecognized mechanism of neurogenesis associated with depression. Our results suggest that: (1) chronic unpredictable stress induces depression-like symptoms, which are accompanied with an inhibition of hippocampal DG neurogenesis in rats, (2) exosomes derived from microglia transport miR-146a-5p to DG regions where they can then regulate neuronal function, (3) miR-146a-5p regulates the neurogenesis linked with depression through the KLF4/CDKL5 pathway, and (4) circANKS1B is involved in the development of depression via the miR-146a-5p signaling pathway. Collectively, these data offer the novel hypothesis that microglia, which secrete exosomes containing miR-146a-5p, play an important role in the neurogenesis that is coupled with depression via the miR-146a-5p/KLF4 pathway (Figure 7). miR-146a-5p may thus represent a new potential therapeutic target for depression.

Emerging findings have indicated the importance of neurogenesis in central nervous system disease and, specifically, depression is closely associated with reduced neurogenesis.⁹ Interestingly, microglial degeneration is also observed in depressed patients.³³ In this study, we established that chronic unpredictable stress effectively induces symptoms of depression in rats and, more importantly, that these behavioral responses were accompanied with alterations in neurogenesis and reductions in neuronal activity within the hippocampal DG area. miRNAs play important roles in neurogenesis and participate in the transition of NSCs from proliferation to differentiation stages.³⁴ Our current study was designed to focus upon key miRNAs that can regulate neurogenesis and their role in the pathology of depression.

The therapeutic potentials of miRNAs are gaining increasing attention of late. In fact, miRNAs have been successfully used in the treatment of cancer,³⁵ and miRNAs as therapeutic agents for depression, have shown some promising results. However, there remains much to work to be done before miRNAs can be utilized as safe and effective

Figure 3. Internalization of microglia-derived exosomes in DG neurons and effects on neuronal differentiation and migration

(A) Relative expression levels of miR-146a-5p in BV-2-derived exosomes. SnRNAU6 as the internal controls. n = 6 per group. **p < 0.01 BV-2-LPS-Exo versus BV-2-untreated-Exo. (B) Representative western blot images of relative protein levels for CD13, MCT-1, CD14, IL-1 β , TMEM119, CD11b, and CD63 in rat serum-derived exosomes. n = 6 per group. *p < 0.05 CUMS-Exo versus Ctrl-Exo. (C) Confocal microscopy images showing internalization of exosomes in DG neurons of the hippocampus. Scale bars, 10 μ m (white), 10 μ m (red). n = 6 per group. (D–F) Exosomes derived from LPS-treated BV-2 cells (LPS/Exo) or GW4869-treated BV-2 cells (GW4869/Exo) were added into the medium. Proliferation (D) and differentiation (E and F) of neuronal stem cells (NSCs) as determined *in vitro* using immunofluorescence. Scale bars, 30 μ m. n = 5 per group. **p < 0.01, ***p < 0.001, ****p < 0.0001 LPS/Exo group (exosomes from LPS-treated BV-2 cells) versus naive group (exosomes from non-LPS- and non-GW4869-treated BV-2 cells), &p < 0.05, &&p < 0.01 LPS/GW4869/Exo group (exosomes from LPS- and GW4869-treated BV-2 cells) versus LPS/Exo group (exosomes from LPS-treated BV-2 cells). Data represent means \pm SEM. Student's t tests for comparisons between the two groups (A and B). One-way ANOVA with Tukey's post hoc test for multiple comparisons involving >2 groups (D–F). Ctrl, control.



(legend on next page)

therapeutic targets for depression, especially with regard to their methods of delivery and capacity for target specificity. Exosomes, which are considered as delivery vectors, can carry specific miRNAs to cell receptors, and play a key role in the pathogenesis of central nervous system diseases.³⁶ As exosomes can cross the blood-brain barrier, they offer a means for achieving a precise delivery of miRNA to its intended central nervous system target. Therefore, given the potential significance of exosomes as related to miRNAs, in this study we assessed the expression profile of miRNAs in exosomes from rat serum. We not only found that a specific miRNA, miR-146a-4p, was closely related to signaling pathways regulating pluripotency of stem cells, but that it was also enriched and significantly increased in the exosomes of CUMS rats. Similar effects are observed in patients with MDD. Accordingly, these data provide clear evidence for the possibility that exosomes containing miR-146a-5p might mediate the development of neurogenesis in depression. As the DG of the adult brain represents a key region for neurogenesis,³⁷ our studies were focused on this site. Interestingly, miR-146a-5p was found to be markedly increased in the DG area of CUMS rats. Based on these results, we hypothesize that exosomes carrying miR-146a-5p are internalized within DG neurons, resulting in their upregulation at this site and, in this way, participate in the neurogenesis associated with depression.

miRNAs have been shown to play important roles in both brain development and regulation of adult neuronal cell functions.³⁸ Interestingly, the brain has a particularly high proportion of tissue-specific and tissue-enriched miRNAs.^{39–42} Neuronal miRNA expression represents a highly specific cell-type process, such as neuronal-enriched miR-376a and astrocyte-enriched miR-21.⁴³ Of particular significance to the present investigation, miR-146a-5p has been shown to be a microglial-enriched miRNA that affects excitatory synapses.^{17,18} Therefore, we postulated that the increased levels of miR-146a-5p found in exosomes of CUMS rats were secreted by microglia. Amino-peptidase CD13 is an important characteristic protein of exosomes derived from microglia,⁴⁴ and high expression of CD13 was observed in the serum-derived exosomes of depressed rats, providing support for this hypothesis. Meanwhile, the increased expression of some other specific markers of microglial exosomes, such as MCT-1, CD14, IL-1 β , TMEM119, and CD11b, further confirmed that the exosomes in serum of CUMS rats are main of microglial origin.

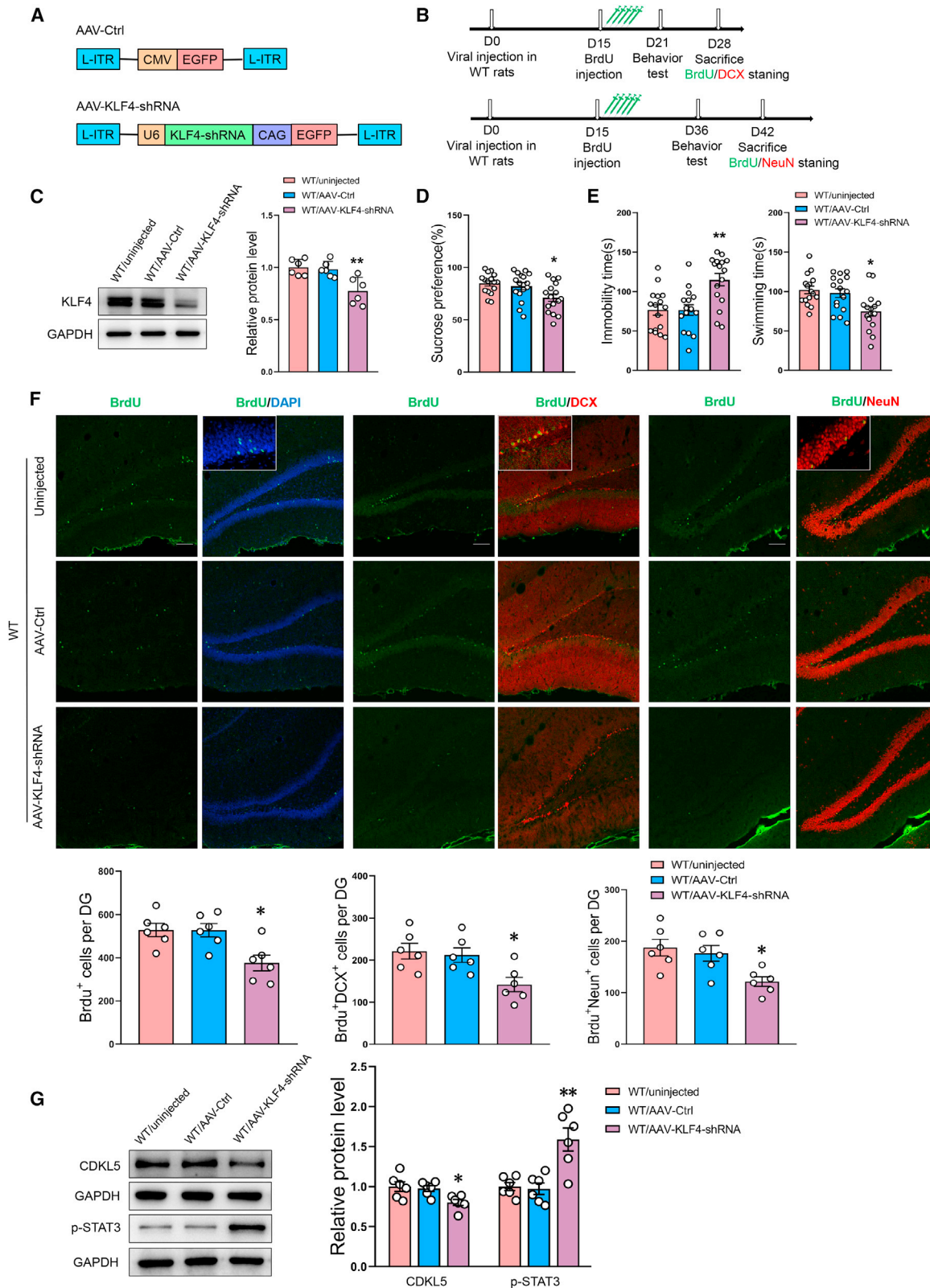
It has been reported that glial-enriched miR-146a-5p can inhibit neuronal differentiation.²⁹ Consistent with previous studies, we found that exosomes containing 146a-5p as secreted by microglia inhibited neuronal differentiation and migration of NSCs. Furthermore, miR-146a-5p suppresses neurogenesis in the DG region of the hippocampus, thereby enhancing depression-like behaviors. However, details regarding molecular mechanisms through which miR-146a-5p regulates neurogenesis in the DG region require further investigation.

A single miRNA can target hundreds of mRNAs to regulate a variety of pathophysiological processes.^{45,46} As one example, miR-124 can regulate neurogenesis by targeting Dlx2⁴⁷ and Sp1 to regulate the differentiation of mesenchymal stem cells.⁴⁸ It has been reported that the expression of KLF4 in neural stem cells can regulate the differentiation and migration of neurons in the developing cerebral cortex.²⁸ Here, we demonstrate that KLF4 does, in fact, interact with miR-146a-5p, effects corroborated from results as obtained with *in vivo* experiments. KLF4 can specifically bind to the phosphorylated forms of STAT3 (p-STAT3) and inhibit its expression.³⁰ In addition, cyclin-dependent kinase-like 5 (CDKL5) is highly expressed in the brain and deficiencies in CDKL5 inhibit the formation of new granular neurons.³¹ In this study, miR-146a-5p appears to bind with KLF4 to inhibit the expression of CDKL5 and increase STAT3 phosphorylation levels, thereby reducing neurogenesis and inducing depression-like behaviors. KLF4 silencing induces depression-like behaviors and, consistent with previous studies, induces deficiencies in the development of new neurons. Taken together, these data demonstrate that miR-146a-5p derived from microglia-generated exosomes appears to provide a bridge between stress exposure and neurogenesis. More specifically, linking of the KLF4/P-STAT3/CDKL5 pathway, as regulated by miR-146a-5p, appears to be a key factor in the pathogenesis of depression. Whether or not miR-146a-5p regulates the expression of other genes that participate in neurogenesis remains to be determined.

circRNAs are a group of non-coding RNA molecules.⁴⁹ Recently, circRNAs were observed to be highly expressed in neurons and have been associated with neuronal development and synaptic plasticity.⁵⁰ Of particular relevance to our study is the report that abnormal expressions of circRNAs are present in the blood of

Figure 4. MiR-146a-5p in DG regions is associated with depression-like phenotypes and suppression of neurogenesis via the KLF4/CDKL5 pathway

(A) Schematics of AAV vectors engineered to overexpress miR-146a-5p or knockdown miR-146a-5p and their corresponding controls. (B) Experimental paradigm for determining behavioral responses of rats infected with the virus. (C) Illustration of viral infusion into the rat DG regions. Scale bars, 2 mm (red), 20 μ m (white). (D and E) Behavioral effects of expressing various viral constructs in DG regions as shown for the sucrose preference test (SPT) (D) and forced swim test (FST) (E). n = 18 per group. *p < 0.05, **p < 0.01 WT/AAV-miR-146a-5p versus WT/AAV-Ctrl, [§]p < 0.05, ^{§§}p < 0.01 CUMS/AAV-miR-146a-5pi versus CUMS/AAV-Ctrl. (F) Representative confocal microscopic images of immunostainings for DCX⁺ and Nestin⁺ cells in the DG regions. Scale bars, 50 μ m. n = 6 per group. *p < 0.05, **p < 0.01 WT/AAV-miR-146a-5p versus WT/AAV-Ctrl, [§]p < 0.05 CUMS/AAV-miR-146a-5pi versus CUMS/AAV-Ctrl. (G) Representative traces of sEPSC in DG neurons of rats infected with the virus. (H and I) Cumulative fraction plots of sEPSC amplitudes (H) and frequencies (I) in neurons of rat DG regions. n = 16 neurons from 6 WT/AAV-Ctrl rats, n = 16 neurons from 7 WT/AAV-miR-146a-5p rats, n = 18 neurons from 6 CUMS/AAV-Ctrl rats, and n = 18 neurons from 6 CUMS/AAV-miR-146a-5pi rats. **p < 0.01 WT/AAV-miR-146a-5p versus WT/AAV-Ctrl, [§]p < 0.05, ^{§§}p < 0.01 CUMS/AAV-miR-146a-5pi versus CUMS/AAV-Ctrl. (J) Representative western blot images showing relative protein levels of KLF4 and CDKL5, and phosphorylation of STAT3 in AAV-miR-146a-5p-infected DGs of WT rats. n = 6 per group. *p < 0.05 WT/AAV-miR-146a-5p versus WT/AAV-Ctrl. (K) Representative western blot images showing relative protein levels of KLF4 and CDKL5, and phosphorylation of STAT3 in AAV-miR-146a-5p-infected DGs of CUMS rats. n = 6 per group. [§]p < 0.05 CUMS/AAV-miR-146a-5pi versus CUMS/AAV-Ctrl rat. Data represent means \pm SEM. One-way ANOVA with Tukey's post hoc test for multiple comparisons involving >2 groups (D–F, H–K). Ctrl, control.



(legend on next page)

MDD patients.⁵¹ Therefore, we used high-throughput sequencing to establish that circRNAs are involved in MDD. We also observed that circAnka1b, as an exonic circular RNA, was notably decreased in the DG region of CUMS rats. It is well known that miRNAs play a key role in post-transcriptional regulation and circRNAs function as miRNA sponges to modulate the pathogenesis and progression of various diseases.^{32,52} For example, a circRNA derived from the Sry transcript sequesters miR-138 in the testes,⁵³ while circRNA Cdr1binds miR-7 and miR-671 to regulate synaptic transmission.⁵² We speculated that circANKS1B might competitively bind with miR-146a-5p to relieve its inhibitory effects on associated target genes. Results as obtained in *in vivo* experiments have verified that circANKS1B binds to miR-146a-5p to reverse reductions in KLF4 protein. Moreover, silencing circANKS1B significantly attenuated neurogenesis and induced depression-like symptoms in normal rats, while an overexpression of circANKS1B enhanced DG neurogenesis and ameliorated depression-like behaviors in CUMS rats. In this way, we present the first evidence identifying a function for circANKS1B in the regulation of neurogenesis and behavior in rats with chronic stress, via the capacity for circANKS1B to function as an absorbing agent. However, details regarding information on the mechanisms and functional roles of circRNAs in neurological diseases, which will be needed for the development of novel candidate drugs for disease treatments, will require further investigation.

It should be pointed out that this study mainly investigated whether microglia-derived miR-146a-5p-containing exosomes can function as a critical factor to regulate neurogenesis in depression and suggests that microglial exosomes act as a new crosstalk channel between glial cells and neurons. However, there are still some limitations. Firstly, the present study lacks definitive proof to confirm the glia-to-neuron shuttling of bioactive miR-146a-5p via exosomes. Despite recent advances in exosome research, how to deliver the cargo of extracellular vesicles⁴⁰ to target cells remains largely unclear. Secondly, this study demonstrated that miR-146a-5p was mainly derived from exosomes released by microglia, and overexpressing miR-146a-5p could down-regulate the expression level of KLF4. However, whether the decreased KLF4 in the depression model is mediated by miR-146a-5p from microglia-derived exosomes needs further confirmation. In addition, chronic social stress has been shown to induce glucocorticoid-mediated pro-inflammatory response and pyramidal dendrite retraction in the hippocampus.⁵⁴ However, there are differences in function and mechanisms between the LPS-induced inflammation *in vitro* and chronic stress-induced inflammation *in vivo*. So, further study remains to clarify whether LPS stimulation could functionally

regulate neurogenesis via the HPA axis. In addition, a miRNA usually has hundreds of target genes, and previous studies have reported that IRAK1 and TRAF6 are also the most highly conserved targets of miR-146a-5p.^{55,56} Therefore, it is interesting to further investigate the comprehensive mechanisms of miR-146a-5p in depression.

In conclusion, the findings presented in this report represent the first evidence showing that miR-146a-5p is involved in the crosstalk between microglial exosomes and neurogenesis in depression. miR-146a-5p, which is enriched in microglia-derived exosomes, is shuttled to DG neurons, leading to an inhibition of neurogenesis by affecting the target gene, KLF4. In addition, we demonstrate that circANKS1B mediates miR-146a-5p regulation of KLF4 mRNA expression and its functional involvement in the neurogenesis of depression. In this way, our results reveal that microglia-derived miR-146a-5p can function as a crucial signaling mediator during neurogenesis in depression and indicate a novel role for miR-146a-5p as a therapeutic target in depression. Taken together, these observations suggest that targeting the neurogenesis involved with depression may provide a new avenue for the development of novel therapeutic strategies in the treatment of depression.

MATERIALS AND METHODS

Animals

Male Wistar rats (120–140 g) were purchased from the animal center of Shandong University. All experimental procedures were reviewed and approved by the Ethics Committee of Shandong College (ECSBMSSDU2020-2-017), and strictly abide by the International Guiding Principles of Animal Research formulated by the Council of the International Medical Science Organization. Additional information regarding the care and maintenance of these rats is contained in the [supplemental information](#).

CUMS model

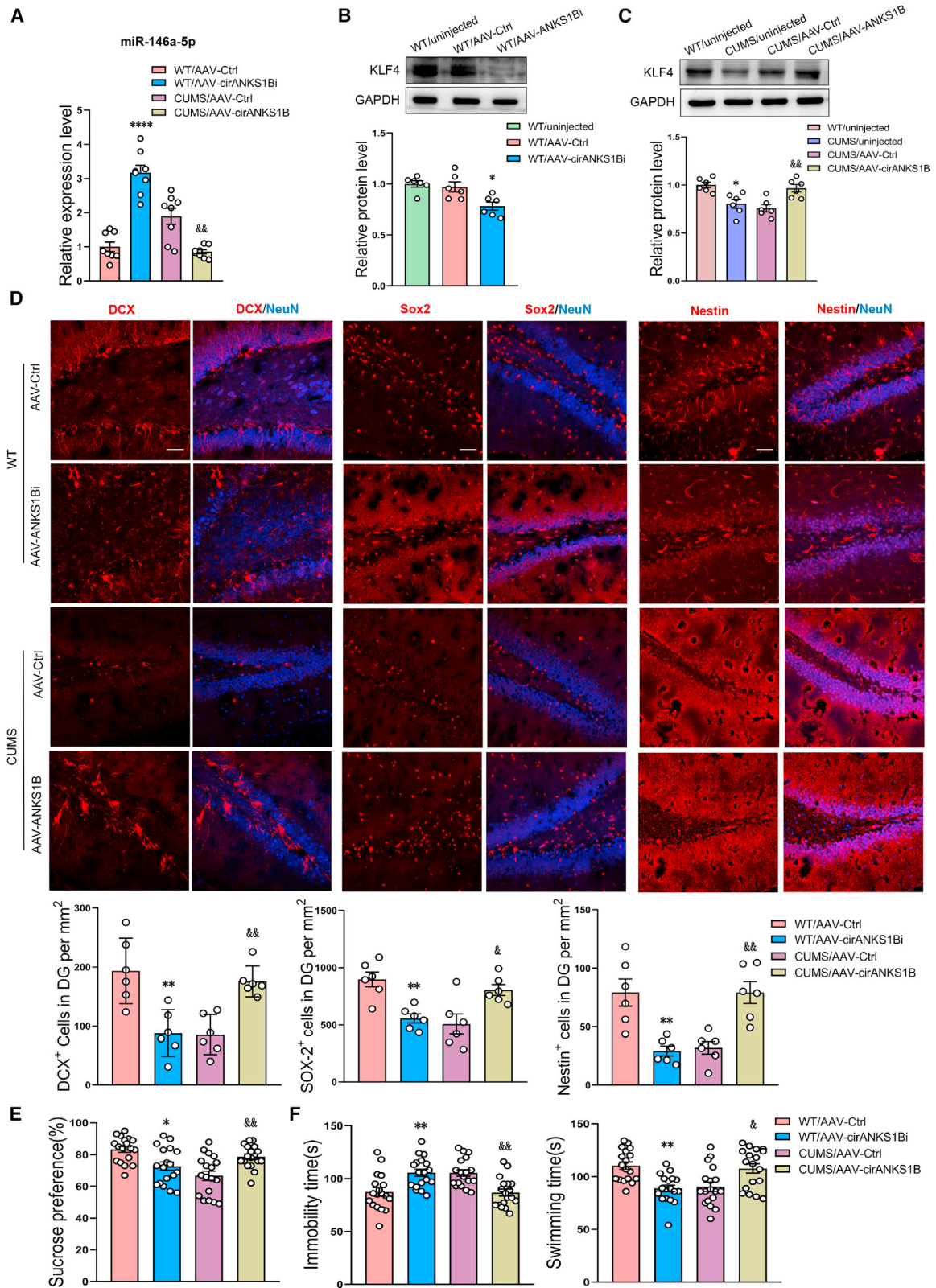
Details regarding procedures for inducing the CUMS-induced rat model of depression have been described previously with slight modifications.⁵⁷ In brief, after 7 days of adaption to the laboratory conditions, rats were exposed to a variable sequence of stressors in a random sequence for 5 weeks. Descriptions of the types of stressors applied in this study and behavioral tests used to assess depression are contained in the [supplemental information](#).

Stereotaxic injection of the adeno-associated virus

The adeno-associated virus (AAV) virus used for stereotaxic injections was obtained from GENEchem (Shanghai, China). For viral

Figure 5. Blocking KLF4 in DG regions induces depression-like behaviors in normal rats and inhibits neurogenesis through the P-STAT3/CDKL5 pathway

(A) Schematics of AAV vectors engineered to knock down KLF4 and their corresponding controls. (B) Experimental paradigm for determining behavioral responses of rats infected with the virus and BrdU. (C) Representative western blot images showing the knockdown efficiency of KLF4. $n = 6$ per group. $**p < 0.01$ WT/AAV-KLF4-shRNA versus WT/AAV-Ctrl rats. (D and E) Behavioral responses in the SPT (D) and FST (E) of rats with knockdown of viral AAV-KLF4-shRNA in the DG regions. $n = 16$ per group. $*p < 0.05$, $**p < 0.01$ WT/AAV-KLF4-shRNA versus WT/AAV-Ctrl rats. (F) Representative confocal microscopic images of immunostainings for cell numbers of BrdU⁺, BrdU⁺/DCX⁺, and BrdU⁺/NeuN⁺ in the DG. Scale bars, 50 μm . $n = 6$ per group. $*p < 0.05$ WT/AAV-KLF4-shRNA versus WT/AAV-Ctrl rats. (G) Representative western blot images showing relative protein levels of CDKL5 and phosphorylation of STAT3 in virus-infected DGs. $n = 6$ per group. $*p < 0.05$, $**p < 0.01$ WT/AAV-KLF4-shRNA versus WT/AAV-Ctrl rats. Data represent means \pm SEM. One-way ANOVA with Tukey's post hoc test for multiple comparisons involving >2 groups (C–G). WT, wild type; Ctrl, control.



(legend on next page)

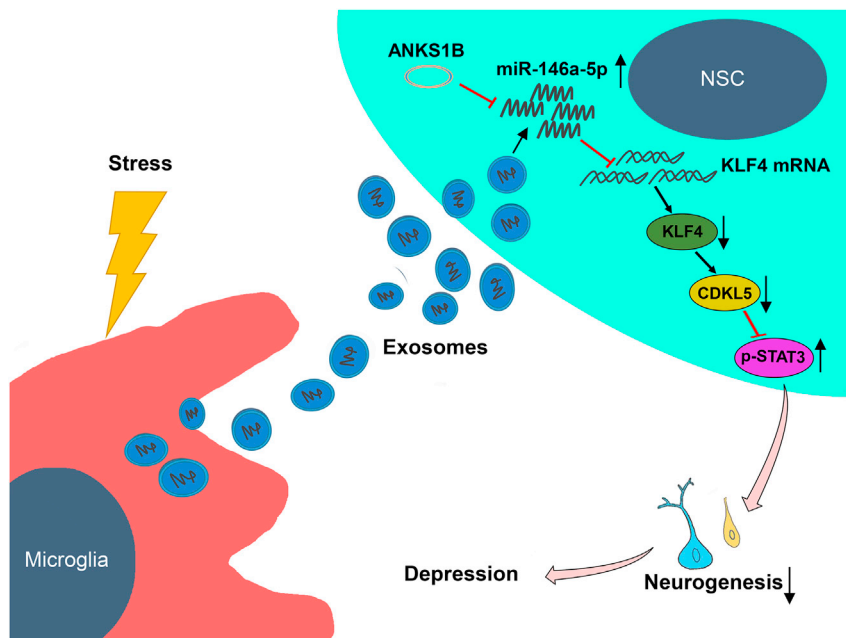


Figure 7. Stress-triggered microglia secrete exosomes containing miR-146a-5p to regulate neurogenesis via the miR-146a-5p/KLF4 signaling pathway in depression

ANKS1B, circRNA-ANKS1B; NSC, neural stem cell.

injection, rats were anesthetized with 2.5% isoflurane and then placed in a stereotaxic frame. Purified and concentrated AAV virus ($\sim 10^{12}$ infection units per mL) was injected bilaterally in a volume of 2.0–2.5 μL into the hippocampal DG region using an electric microinjection pump (Stoelting, USA) at a rate of 150 nL/min. The site of viral injections was verified according to the Rat Brain Atlas for Wistar rats using the following coordinates: from the bregma, -3.24 mm; medial/lateral, ± 1.7 mm; dorsal/ventral, -3.5 mm. Behavioral experiments or biochemical assays were performed at a minimum of 14 days after surgery. Injection sites were verified after behavioral tests and only data from rats with correct injection site placements were used for subsequent experiments.

Hippocampal slice preparations and electrophysiological recordings

Hippocampal slices (400 μm thick) were prepared according to procedures described previously.⁵⁸ In brief, coronal slices were sectioned using a vibratome (VT-1000, Leica) in oxygenated ice-cold cutting solution. Slices were then transferred as quickly as possible to a recovery solution for 30 min at 30°C. The slices were allowed a minimum recovery period of 1 h at room temperature

before recording. Whole-cell patch-clamp recordings were performed in DG granule cells. The glass micropipettes (4–6 M Ω) were filled with an internal solution. During recordings, slices were continuously perfused with an artificial cerebral spinal fluid at a temperature of 31°C–33°C and flow rate of ~ 2 mL/min. Cells were visualized with infrared optics on an upright microscope (BX51WI, Olympus). A MultiClamp 700B amplifier and pCLAMP10 software were used to record the electrophysiological responses (Axon Instruments). sEPSCs were recorded at a holding potential of -70 mV with 50 μM picrotoxin in the ASCF. Results were analyzed using a Mini Analysis Program and all the chemicals used in these electrophysiological recordings were purchased from Sigma. Additional details regarding these solutions are contained in the [supplemental information](#).

Additional assays/procedures

Immunofluorescence, western blotting, cell cultures, dual luciferase assay, lentivirus transfection, flow cytometry, exosome labeling, and quantitative real-time PCR were performed as described detail in the [supplemental information](#). The accession number of the RNA-seq data reported in this paper is GEO: GSE185777.

Figure 6. circANKS1B regulates neurogenesis in the DG region through the miR-146a-5p/KLF4 pathway

(A) Relative expression levels of miR-146a-5p in DG regions infected with the AAV-circANKS1B-shRNA or the AAV-circANKS1B virus. $n = 6$ per group. **** $p < 0.0001$ WT/AAV-circANKS1Bi versus WT/AAV-Ctrl, $\&\&p < 0.01$ CUMS/AAV-circANKS1B versus CUMS/AAV-Ctrl. (B and C) Representative western blot images showing relative protein levels of KLF4 in DG regions infected with the AAV-circANKS1B-shRNA (B) or the AAV-circANKS1B (C) virus. $n = 6$ per group. * $p < 0.05$ WT/AAV-circANKS1Bi versus WT/AAV-Ctrl, $\&\&p < 0.01$ CUMS/AAV-circANKS1B versus CUMS/AAV-Ctrl. (D) Representative confocal microscopic images of immunostainings for DCX⁺, Sox2⁺, and Nestin⁺ cells in DG regions infected with the virus. Scale bars, 50 μm . $n = 6$ per group. ** $p < 0.01$ WT/AAV-circANKS1Bi versus WT/AAV-Ctrl, $\&p < 0.05$, $\&\&p < 0.01$ CUMS/AAV-circANKS1B versus CUMS/AAV-Ctrl. (E and F) Behavioral responses in the SPT (E) and FST (F) of rats with expression of the AAV-circANKS1B-shRNA construct in the DG of WT rats and the AAV-circANKS1B construct in the DG of CUMS rats. $n = 18$ per group. * $p < 0.05$, ** $p < 0.01$ WT/AAV-circANKS1Bi versus WT/AAV-Ctrl, $\&p < 0.05$, $\&\&p < 0.01$ CUMS/AAV-circANKS1B versus CUMS/AAV-Ctrl. Data represent means \pm SEM. One-way ANOVA with Tukey's post hoc test for multiple comparisons involving > 2 groups (A–F). WT, wild type; Ctrl, control.

Statistical analysis

All data are expressed as the means \pm SEM and analyses performed with GraphPad Prism 8.0 (GraphPad Software, La Jolla, CA, USA) for statistical analysis. Student's *t* tests were employed for comparisons between two groups, while a one-way analysis of variance⁵⁹ was used to establish differences among >2 groups with the Tukey's test for post hoc comparisons. Normality between group samples were assessed using the D'Agostino and Pearson omnibus normality test and Brown-Forsythe tests. When normality between sample groups was achieved, one-way ANOVA (followed by Bonferroni's multiple comparisons test), or Student's *t* test were used. Where normality of samples failed, Kruskal-Wallis one-way ANOVA (followed by Dunn's correction), or Mann-Whitney test were performed. All statistical tests were two-tailed and a $p < 0.05$ was required for results to be considered as statistically significant.

DATA AVAILABILITY

The data that support the findings of this study are available from the corresponding author upon reasonable request.

SUPPLEMENTAL INFORMATION

Supplemental information can be found online at <https://doi.org/10.1016/j.ymthe.2021.11.006>.

ACKNOWLEDGMENTS

This study was supported by grants to S.Y.Y. from the National Natural Science Foundation of China (NSFC81873796; 82071513), the Natural Science Foundation of Shandong Province of China (ZR2020ZD25), and the Fundamental Research Funds of Shandong University (2018JC008). We thank Translational Medicine Core Facility of Shandong University for consultation and instrument availability that supported this work.

AUTHOR CONTRIBUTIONS

C.F. designed and conducted *in vivo* experiments, performed data analysis, and assisted in writing the manuscript. Y.L. performed and analyzed the electrophysiological experiments. T.L. and W.W. prepared the rat model of depression. Y.L. conducted *in vitro* experiments. S.Y.Y. designed and directed the experiments, wrote the manuscript, and approved the final version of the manuscript for publication.

DECLARATION OF INTERESTS

The authors declare no competing interests.

REFERENCES

- Malhi, G.S., Coulston, C.M., Fritz, K., Lampe, L., Bargh, D.M., Ablett, M., Lyndon, B., Sapsford, R., Theodoros, M., Woolfall, D., et al. (2014). Unlocking the diagnosis of depression in primary care: which key symptoms are GPs using to determine diagnosis and severity? *Aust. N. J. Psychiatry* 48, 542–547.
- Malhi, G.S., and Mann, J.J. (2018). Depression. *Lancet* 392, 2299–2312.
- Wong, C.H., Siah, K.W., and Lo, A.W. (2019). Estimation of clinical trial success rates and related parameters. *Biostatistics* 20, 366.
- Willner, P. (2005). Chronic mild stress (CMS) revisited: consistency and behavioural-neurobiological concordance in the effects of CMS. *Neuropsychobiology* 52, 90–110.
- Schmaal, L., Hibar, D.P., Samann, P.G., Hall, G.B., Baune, B.T., Jahanshad, N., Cheung, J.W., van Erp, T.G.M., Bos, D., Ikram, M.A., et al. (2017). Cortical abnormalities in adults and adolescents with major depression based on brain scans from 20 cohorts worldwide in the ENIGMA Major Depressive Disorder Working Group. *Mol. Psychiatry* 22, 900–909.
- Kempton, M.J., Salvador, Z., Munafo, M.R., Geddes, J.R., Simmons, A., Frangou, S., and Williams, S.C.R. (2011). Structural neuroimaging studies in major depressive disorder meta-analysis and comparison with bipolar disorder. *Arch. Gen. Psychiatry* 68, 675–690.
- Boldrini, M., Fulmore, C.A., Tartt, A.N., Simeon, L.R., Pavlova, I., Poposka, V., Rosoklija, G.B., Stankov, A., Arango, V., Dwork, A.J., et al. (2018). Human hippocampal neurogenesis persists throughout aging. *Cell Stem Cell* 22, 589.
- Cole, J., Costafreda, S.G., McGuffin, P., and Fu, C.H.Y. (2011). Hippocampal atrophy in first episode depression: a meta-analysis of magnetic resonance imaging studies. *J. Affect Disord.* 134, 483–487.
- Boldrini, M., Santiago, A.N., Hen, R., Dwork, A.J., Rosoklija, G.B., Tamir, H., Arango, V., and Mann, J.J. (2013). Hippocampal granule neuron number and dentate gyrus volume in antidepressant-treated and untreated major depression. *Neuropsychopharmacology* 38, 1068–1077.
- Fossati, P., and Boyer, P. (2004). Relevance of neuroplasticity and cellular resilience in bipolar disorder and depression: evidence from neuroimaging and cognitive studies. *Eur. Neuropsychopharm.* 14, S123.
- Willner, P., Scheel-Kruger, J., and Belzung, C. (2013). The neurobiology of depression and antidepressant action. *Neurosci. Biobehav. Rev.* 37, 2331–2371.
- Saadatpour, L., Fadaee, E., Fadaei, S., Mansour, R.N., Mohammadi, M., Mousavi, S.M., Goodarzi, M., Verdi, J., and Mirzaei, H. (2016). Glioblastoma: exosome and microRNA as novel diagnosis biomarkers. *Cancer Gene Ther.* 23, 415–418.
- Fruhbeis, C., Frohlich, D., and Kramer-Albers, E.M. (2012). Emerging roles of exosomes in neuron-glia communication. *Front Physiol.* 3, 119.
- Xu, B., Zhang, Y., Du, X.F., Li, J., Zi, H.X., Bu, J.W., Yan, Y., Han, H., and Du, J.L. (2017). Neurons secrete miR-132-containing exosomes to regulate brain vascular integrity. *Cell Res.* 27, 882–897.
- Valadi, H., Ekstrom, K., Bossios, A., Sjostrand, M., Lee, J.J., and Lotvall, J.O. (2007). Exosome-mediated transfer of mRNAs and microRNAs is a novel mechanism of genetic exchange between cells. *Nat. Cell Biol.* 9, 654–U672.
- Cope, E.C., and Gould, E. (2019). Adult neurogenesis, glia, and the extracellular matrix. *Cell Stem Cell* 24, 690–705.
- McNeill, E., and Van Vactor, D. (2012). MicroRNAs shape the neuronal landscape. *Neuron* 75, 363–379.
- Prada, I., Gabrielli, M., Turola, E., Iorio, A., D'Arrigo, G., Parolisi, R., De Luca, M., Pacifici, M., Bastoni, M., Lombardi, M., et al. (2018). Glia-to-neuron transfer of miRNAs via extracellular vesicles: a new mechanism underlying inflammation-induced synaptic alterations. *Acta Neuropathol.* 135, 529–550.
- Sierra, A., Encinas, J.M., Deudero, J.J.P., Chancey, J.H., Enikolopov, G., Overstreet-Wadiche, L.S., Tsirka, S.E., and Maletic-Savatic, M. (2010). Microglia shape adult hippocampal neurogenesis through apoptosis-coupled phagocytosis. *Cell Stem Cell* 7, 483–495.
- Budnik, V., Ruiz-Canada, C., and Wendler, F. (2016). Extracellular vesicles round off communication in the nervous system. *Nat. Rev. Neurosci.* 17, 160–172.
- Nowak, J.S., and Michlewski, G. (2013). miRNAs in development and pathogenesis of the nervous system. *Biochem. Soc. Trans.* 41, 815–820.
- Long, J.M., Ray, B., and Lahiri, D.K. (2012). MicroRNA-153 physiologically inhibits expression of amyloid-beta precursor protein in cultured human fetal brain cells and is dysregulated in a subset of Alzheimer disease patients. *J. Biol. Chem.* 287, 31298–31310.
- Long, J.M., Ray, B., and Lahiri, D.K. (2014). MicroRNA-339-5p down-regulates protein expression of beta-site amyloid precursor protein-cleaving enzyme 1 (BACE1) in human primary brain cultures and is reduced in brain tissue specimens of Alzheimer disease subjects. *J. Biol. Chem.* 289, 5184–5198.
- Cao, D.D., Li, L., and Chan, W.Y. (2016). MicroRNAs: key regulators in the central nervous system and their implication in neurological diseases. *Int. J. Mol. Sci.* 17, 842.

25. Xiao, Y., Guan, J.X., Ping, Y.Y., Xu, C.H., Huang, T., Zhao, H.Y., Fan, H.H., Li, Y.Q., Lv, Y.L., Zhao, T.T., et al. (2012). Prioritizing cancer-related key miRNA-target interactions by integrative genomics. *Nucleic Acids Res.* *40*, 7653–7665.
26. Lopez, J.P., Fiori, L.M., Cruceanu, C., Lin, R., Labonte, B., Cates, H.M., Heller, E.A., Vialou, V., Ku, S.M., Gerald, C., et al. (2017). MicroRNAs 146a/b-5 and 425-3p and 24-3p are markers of antidepressant response and regulate MAPK/Wnt-system genes. *Nat. Commun.* *8*, 15497.
27. Lucanic, M., Plummer, W.T., Chen, E., Harke, J., Foulger, A.C., Onken, B., Coleman-Hulbert, A.L., Dumas, K.J., Guo, S.Z., Johnson, E., et al. (2017). Impact of genetic background and experimental reproducibility on identifying chemical compounds with robust longevity effects. *Nat. Commun.* *8*, 14256.
28. Cui, D.M., Zeng, T., Ren, J., Wang, K., Jin, Y., Zhou, L., and Gao, L. (2017). KLF4 knockdown attenuates TBI-induced neuronal damage through p53 and JAK-STAT3 signaling. *CNS Neurosci. Ther.* *23*, 106–118.
29. Jovicic, A., Roshan, R., Moiso, N., Pradervand, S., Moser, R., Pillai, B., and Luthi-Carter, R. (2013). Comprehensive expression analyses of neural cell-type-specific miRNAs identify new determinants of the specification and maintenance of neuronal phenotypes. *J. Neurosci.* *33*, 5127–5137.
30. Gu, H., Li, Q.D., Huang, S., Lu, W.G., Cheng, F.Y., Gao, P., Wang, C., Miao, L., Mei, Y.D., and Wu, M.A. (2015). Mitochondrial E3 ligase March5 maintains stemness of mouse ES cells via suppression of ERK signalling. *Nat. Commun.* *6*, 7112.
31. Fuchs, C., Trazzi, S., Torricella, R., Viggiano, R., De Franceschi, M., Amendola, E., Gross, C., Calza, L., Bartesaghi, R., and Ciani, E. (2014). Loss of CDKL5 impairs survival and dendritic growth of newborn neurons by altering AKT/GSK-3 beta signaling. *Neurobiol. Dis.* *70*, 53–68.
32. Piwecka, M., Glazar, P., Hernandez-Miranda, L.R., Memczak, S., Wolf, S.A., Rybak-Wolf, A., Filipchuk, A., Klironomos, F., Jara, C.A.C., Fenske, P., et al. (2017). Loss of a mammalian circular RNA locus causes miRNA deregulation and affects brain function. *Science* *357*, eaam8526.
33. Brites, D., and Fernandes, A. (2015). Neuroinflammation and depression: microglia activation, extracellular microvesicles and microRNA dysregulation. *Front Cell Neurosci.* *9*, 476.
34. Marangon, D., Raffaele, S., Fumagalli, M., and Lecca, D. (2019). MicroRNAs change the games in central nervous system pharmacology. *Biochem. Pharmacol.* *168*, 162–172.
35. Hayes, J., Peruzzi, P.P., and Lawler, S. (2014). MicroRNAs in cancer: biomarkers, functions and therapy. *Trends Mol. Med.* *20*, 460–469.
36. Tsilioni, I., Panagiotidou, S., and Theoharides, T.C. (2014). Exosomes in neurologic and psychiatric disorders. *Clin. Ther.* *36*, 882–888.
37. Cameron, H.A., and McKay, R.D.G. (2001). Adult neurogenesis produces a large pool of new granule cells in the dentate gyrus. *J. Comp. Neurol.* *435*, 406–417.
38. Bartel, D.P. (2009). MicroRNAs: target recognition and regulatory functions. *Cell* *136*, 215–233.
39. Lagos-Quintana, M., Rauhut, R., Yalcin, A., Meyer, J., Lendeckel, W., and Tuschl, T. (2002). Identification of tissue-specific microRNAs from mouse. *Curr. Biol.* *12*, 735–739.
40. Kim, J., Krichevsky, A., Grad, Y., Hayes, G.D., Kosik, K.S., Church, G.M., and Ruvkun, G. (2004). Identification of many microRNAs that copurify with polyribosomes in mammalian neurons. *Proc. Natl. Acad. Sci. U S A* *101*, 360–365.
41. Smirnova, L., Grafe, A., Seiler, A., Schumacher, S., Nitsch, R., and Wulczyn, F.G. (2005). Regulation of miRNA expression during neural cell specification. *Eur. J. Neurosci.* *21*, 1469–1477.
42. Sempere, L.F., Freemantle, S., Pitha-Rowe, I., Moss, E., Dmitrovsky, E., and Ambros, V. (2004). Expression profiling of mammalian microRNAs uncovers a subset of brain-expressed microRNAs with possible roles in murine and human neuronal differentiation. *Genome Biol.* *5*, R13.
43. Jorgensen, H.F., Terry, A., Beretta, C., Pereira, C.F., Leleu, M., Chen, Z.F., Kelly, C., Merkschlager, M., and Fisher, A.G. (2009). REST selectively represses a subset of RE1-containing neuronal genes in mouse embryonic stem cells. *Development* *136*, 715–721.
44. Potolicchio, A., Carven, G.J., Xu, X.N., Stipp, C., Riese, R.J., Stern, L.J., and Santambrogio, L. (2005). Proteomic analysis of microglia-derived exosomes: metabolic role of the aminopeptidase CD13 in neuropeptide catabolism. *J. Immunol.* *175*, 2237–2243.
45. Long, J.M., Maloney, B., Rogers, J.T., and Lahiri, D.K. (2019). Novel upregulation of amyloid-beta precursor protein (APP) by microRNA-346 via targeting of APP mRNA 5'-untranslated region: implications in Alzheimer's disease. *Mol. Psychiatry* *24*, 345–363.
46. Hu, W.J., Wen, L., Cao, F., and Wang, Y.X. (2019). Down-regulation of Mir-107 worsens spatial memory by suppressing SYK expression and inactivating NF-KB signaling pathway. *Curr. Alzheimer Res.* *16*, 135–145.
47. Cheng, L.C., Pastrana, E., Tavazoie, M., and Doetsch, F. (2009). miR-124 regulates adult neurogenesis in the subventricular zone stem cell niche. *Nat. Neurosci.* *12*, 399–408.
48. Mondanizadeh, M., Arefian, E., Mosayebi, G., Saidijam, M., Khansarinejad, B., and Hashemi, S.M. (2015). MicroRNA-124 regulates neuronal differentiation of mesenchymal stem cells by targeting Sp1 mRNA. *J. Cell Biochem.* *116*, 943–953.
49. Kawashima, H., Numakawa, T., Kumamaru, E., Adachi, N., Mizuno, H., Ninomiya, M., Kunugi, H., and Hashido, K. (2010). Glucocorticoid attenuates brain-derived neurotrophic factor-dependent upregulation of glutamate receptors via the suppression of microRNA-132 expression. *Neuroscience* *165*, 1301–1311.
50. You, X.T., Vlatkovic, I., Babic, A., Will, T., Epstein, I., Tushev, G., Akbalik, G., Wang, M.T., Glock, C., Quedenau, C., et al. (2015). Neural circular RNAs are derived from synaptic genes and regulated by development and plasticity. *Nat. Neurosci.* *18*, 603.
51. Jiang, G.J., Ma, Y., An, T., Pan, Y.Y., Mo, F.F., Zhao, D.D., Liu, Y.F., Miao, J.N., Gu, Y.J., Wang, Y.G., et al. (2017). Relationships of circular RNA with diabetes and depression. *Sci. Rep.* *7*, 7285.
52. Cheng, X.F., Zhang, L., Zhang, K., Zhang, G.Y., Hu, Y., Sun, X.J., Zhao, C.Q., Li, H., Li, Y.M., and Zhao, J. (2018). Circular RNA VMA21 protects against intervertebral disc degeneration through targeting miR-200c and X linked inhibitor-of-apoptosis protein. *Ann. Rheum. Dis.* *77*, 770–779.
53. Hansen, T.B., Jensen, T.I., Clausen, B.H., Bramsen, J.B., Finsen, B., Damgaard, C.K., and Kjems, J. (2013). Natural RNA circles function as efficient microRNA sponges. *Nature* *495*, 384–388.
54. Frodl, T., and Amico, F. (2014). Is there an association between peripheral immune markers and structural/functional neuroimaging findings? *Prog. Neuropsychopharmacol. Biol. Psychiatry* *48*, 295–303.
55. Wu, H., Fan, H., Shou, Z., Xu, M., Chen, Q., Ai, C., Dong, Y., Liu, Y., Nan, Z., Wang, Y., et al. (2019). Extracellular vesicles containing miR-146a attenuate experimental colitis by targeting TRAF6 and IRAK1. *Int. Immunopharmacol.* *68*, 204–212.
56. Iacona, J.R., and Lutz, C.S. (2019). miR-146a-5p: expression, regulation, and functions in cancer. *Wiley Interdiscip. Rev. RNA* *10*, e1533.
57. Wang, P., Feng, Y.B., Wang, L.Y., Li, Y., Fan, C.Q., Song, Q.Q., and Yu, S.Y. (2019). Interleukin-6: its role and mechanisms in rescuing depression-like behaviors in rat models of depression. *Brain Behav. Immun.* *82*, 106–121.
58. Li, N., Cui, L., Song, G., Guo, L., Gu, H.T., Cao, H.S., Li, G.D., and Zhou, Y. (2018). Adolescent isolation interacts with DISC1 point mutation to impair adult social memory and synaptic functions in the hippocampus. *Front Cell Neurosci.* *12*, 238.
59. Alexander, R.C., Cabirac, G., Lowenkopf, T., Casanova, M.F., Kleinman, J., Wyatt, R.J., and Kirch, D.G. (1992). Search for evidence of herpes-simplex virus, type-1, or varicella-zoster virus-infection in postmortem brain-tissue from schizophrenic-patients. *Acta Psychiatry Scand.* *86*, 418–420.